

Hydroxyindole Carboxylic Acid-Based Inhibitors for Receptor-Type Protein Tyrosine Protein Phosphatase Beta

Li-Fan Zeng,¹ Ruo-Yu Zhang,¹ Yunpeng Bai,¹ Li Wu,² Andrea M. Gunawan,² and Zhong-Yin Zhang¹

Abstract

Aims: Protein tyrosine phosphatases (PTPs) play an important role in regulating a wide range of cellular processes. Understanding the role of PTPs within these processes has been hampered by a lack of potent and selective PTP inhibitors. Generating potent and selective probes for PTPs remains a significant challenge because of the highly conserved and positively charged PTP active site that also harbors a redox-sensitive Cys residue. **Results:** We describe a facile method that uses an appropriate hydroxyindole carboxylic acid to anchor the inhibitor to the PTP active site and relies on the secondary binding elements introduced through an amide-focused library to enhance binding affinity for the target PTP and to impart selectivity against off-target phosphatases. Here, we disclose a novel series of hydroxyindole carboxylic acid-based inhibitors for receptor-type tyrosine protein phosphatase beta (RPTP β), a potential target that is implicated in blood vessel development. The representative RPTP β inhibitor **8b-1** (L87B44) has an IC₅₀ of 0.38 μ M and at least 14-fold selectivity for RPTP β over a large panel of PTPs. Moreover, **8b-1** also exhibits excellent cellular activity and augments growth factor signaling in HEK293, MDA-MB-468, and human umbilical vein endothelial cells. **Innovation:** The bicyclic salicylic acid pharmacophore-based focused library approach may provide a potential solution to overcome the bioavailability issue that has plagued the PTP drug discovery field for many years. **Conclusion:** A novel method is described for the development of bioavailable PTP inhibitors that utilizes bicyclic salicylic acid to anchor the inhibitors to the active site and peripheral site interactions to enhance binding affinity and selectivity. *Antioxid. Redox Signal.* 20, 2130–2140.

Introduction

PROTEIN TYROSINE PHOSPHORYLATION is a major post-translational modification by which many cellular pathways are regulated. In living cells, the proper level of protein tyrosine phosphorylation is fine-tuned and dynamically controlled by the balanced activity of protein tyrosine kinases (PTKs) and protein tyrosine phosphatases (PTPs), which are crucial for cell growth, differentiation, metabolism, motility, and death (16, 29). Understandably, perturbation of this balance leads to many human diseases, including diabetes, cancer, and immune dysfunctions (16, 17, 27, 39), implicating both enzyme classes as highly attractive targets for the development of novel therapeutics (8, 27). Indeed, nearly two dozen of small-molecule drugs targeting PTKs have been approved for the clinic over the past decade, and many more

Innovation

Although the protein tyrosine phosphatases (PTPs) have been garnering attention as potential therapeutic targets, they remain largely an untapped resource. In fact, PTP-based drug discovery programs have historically been shrouded with difficulty in inhibitor selectivity and bioavailability. This study describes a chemistry platform based on bicyclic salicylic acid pharmacophores that are sufficiently polar to bind the PTP active site, yet remain capable of crossing cell membranes, offering PTP inhibitors with both high selectivity and cellular efficacy. Potent and specific PTP inhibitors could serve as valuable tools to illuminate the druggability of PTPs and may constitute valuable therapeutics for many human diseases.

¹Department of Biochemistry and Molecular Biology, Indiana University School of Medicine, Indianapolis, Indiana.

²Chemical Genomics Core Facility, Indiana University School of Medicine, Indianapolis, Indiana.

are undergoing clinical trials (7). However, the therapeutic potential of modulating the activity of PTPs is underexplored despite the fact that several PTPs have been identified as highly promising targets (17, 39). This is rather surprising, as both PTKs and PTPs are equally important for the regulation of cellular functions.

Among the reasons that PTP-based drug discovery still remains an untapped resource is that the PTP active site presents a number of challenges to developing small-molecule inhibitors. First, the PTPs feature an invariant active site cysteine for nucleophilic catalysis (40). Due to the highly positively charged environment in the PTP active site, the side chain of this Cys residue has an extremely low pK_a (~ 5) (41) in comparison to that of a typical thiol group in proteins (~ 8.5). Thus, at physiological conditions, the catalytic Cys exists as a thiolate anion, which not only enhances its nucleophilicity but also renders it susceptible to oxidation. The sensitivity of the active site Cys to oxidation makes the PTPs prime targets of stimulus-induced production of reactive oxygen species (ROS) (2, 9, 20, 24), which inactivate the PTPs, thereby potentiating tyrosine phosphorylation-mediated signaling (14, 19, 25, 33). Thus, the oxidative inactivation of the PTPs by ROS offers a dynamic mechanism of PTP regulation. Unfortunately, the reactivity of the active site Cys also causes serious problems in high throughput screening campaigns that are aimed at the discovery of PTP inhibitory agents, as highly reactive oxidizing and alkylating agents often surface as hits (4, 30), which are undesirable as therapeutics due to poor safety and selectivity profiles. Furthermore, because of the positively charged PTP active site evolved to complement the negatively charged pTyr substrate, the brute-force screening of large compound collections usually leads to the identification of negatively charged molecules that suffer from poor bioavailability. Finally, the PTP active site is structurally very well conserved, so it is not trivial to obtain compounds that can inhibit single PTPs with good selectivity.

One way of circumventing the inhibitor specificity issue is through focused library approaches that link a non-hydrolyzable pTyr mimetic to appropriately functionalized moieties to engage both the PTP active site and its nearby peripheral binding pockets which are less conserved (28, 40). To improve the pharmacological properties of PTP inhibitory agents, we discovered that bicyclic hydroxybenzofuran and hydroxyindole carboxylic acid scaffolds can serve as effective nonhydrolyzable pTyr mimics and are sufficiently polar to bind the PTP active site, yet remain capable of crossing cell membranes (35, 38, 42). We demonstrated that hydroxybenzofuran or indole-based carboxylic acids bind the PTP active site in an analogous fashion as pTyr, but additional diversity elements attached to the benzofuran/indole core interact with unique secondary pockets in the vicinity of the active site and, therefore, render the inhibitors PTP isozyme selective. Click chemistry was initially utilized to tether an alkyne-containing hydroxybenzofuran/indole carboxylic acid scaffold with a large number of azide-containing amines and hydrazines in order to target adjacent secondary binding pockets in the vicinity of the PTP active site. This led to the identification of several PTP inhibitors (35, 38, 42). However, despite the highly efficacious cellular activity, the potency and selectivity displayed by these inhibitors are relatively modest, and, therefore, are not adequate for chemical biological investigation and therapeutic development. The reasons that

the Click chemistry approach did not produce better results may be as follows: (i) the hydroxybenzofuran/indole carboxylic acid cores were not optimized for the intended target PTPs; (ii) the triazole linker resulting from the Click reaction was not most favorable for ligand interactions with the PTPs; and (iii) the presence of cuprous ion used in the Click reaction may compromise on the quality of the identified hits.

To avoid the problems associated with the Click chemistry approach and to develop more potent and selective PTP inhibitors, we decide to first identify the most efficient hydroxyindole carboxylic acid core for the target PTP, which will then be combined with a large and diverse number of carboxylic acids through the well-established amide chemistry in order to target peripheral pockets in the vicinity of the active site. We describe the application of this strategy to the development of potent and selective inhibitors of receptor-type tyrosine protein phosphatase beta (RPTP β) with efficacious cellular activity.

RPTP β , encoded by the *PTPRB* gene in humans, is expressed primarily in endothelial cells that form the protective lining of blood vessels. RPTP β is composed of an extracellular domain with multiple fibronectin type III repeats, a single transmembrane segment, and one cytoplasmic catalytic domain (18). Mice expressing a truncated form of VE-PTP (mouse homolog of human RPTP β) and VE-PTP null mice undergo vasculogenesis but die embryonically as a result of defects in angiogenesis, indicating an important role for VE-PTP in blood vessel development (3, 10). RPTP β can negatively regulate the activation of Tie-2, an endothelial cell-specific receptor PTK, whose activation has been implicated in the development of collateral blood vessels that restore blood flow to ischemic tissue, vascular vessel maintenance, and integrity (6, 11, 12, 32). Antibodies against the extracellular domain of RPTP β mimic the effects of VE-PTP gene deletion, triggering the activation of Tie-2 and leading to enhanced endothelial cell proliferation and enlargement of vascular structures through activation of Erk1/2 (31). A nonspecific phosphatase inhibitor *bis*(maltolato)-oxovanadium (IV) that inhibits RPTP β augments collateral blood flow in a rat model of vascular insufficiency (5). All together, these data suggest that RPTP β plays an important role in blood vessel growth and maintenance, and RPTP β may be a potential target for tumor growth, occlusive cardiovascular disease, vascular leaking syndrome, and other vascular-related diseases. Understandably, there is intense interest in targeting RPTP β for therapeutic development. However, although several RPTP β inhibitors have been reported (1, 15, 21, 26), none exhibit activity inside the cell.

Results

We previously identified a hydroxyindole carboxylic acid as a pTyr mimic for PTPs. Through Click chemistry, a peripheral binding element was attached to the hydroxyindole carboxylic acid core, yielding an SHP2 inhibitor (II-B08) with highly efficacious activity in a number of cell lines as well as in a mouse model bearing KIT/D814V-induced mast cell leukemia (22, 38). Given the favorable pharmacological properties of hydroxyindole carboxylic acid-based PTP inhibitors, we decided to take a focused library approach to transform the hydroxyindole carboxylic acid scaffold into a highly potent and selective RPTP β inhibitor with excellent cellular activity.

TABLE 1. IC₅₀ VALUES (μM) OF 1A-L FOR RPTPβ

Compd	R ¹	IC ₅₀ (μM)
1a	(1,1'-biphenyl)-4-yl	3.6 ± 0.8
1b	Cyclohexyl	9.6 ± 0.6
1c	4-CF ₃ Oph	16 ± 2
1d	4-CF ₃ Ph	24 ± 1
1e	Ph	24 ± 2
1f	3-NH ₂ Ph	25 ± 5
1g	3-CF ₃ Ph	27 ± 2
1h	4-FPh	40 ± 4
1i	3-FPh	56 ± 5
1j	2-CF ₃ Ph	70 ± 10
1k	3-OHPh	90 ± 20
1l	2-FPh	113 ± 4

The IC₅₀ values for RPTPβ were evaluated at pH 7.0 and 25°C using *p*NPP as a substrate.

RPTPβ, receptor-type tyrosine protein phosphatase beta; *p*NPP, *p*-nitrophenyl phosphate.

To identify a suitable hydroxyindole carboxylic acid core for RPTPβ, we introduced a diverse series of substituents to the 2-position of hydroxyindole carboxylic acid. Specifically, compounds 1a-l were designed, synthesized (37) and their inhibitory activity toward RPTPβ was evaluated at pH 7 and 25°C using *p*-nitrophenyl phosphate (*p*NPP) (Table 1). Compound 1a bearing a biphenyl group surfaced as the most potent hydroxyindole carboxylic acid core (IC₅₀ = 3.6 ± 0.8 μM) for RPTPβ. Unfortunately, compound 1a, bearing a biphenyl ring with no functional group on it, was not easily amendable for further chemical modification at the 2-position. However, compound 1f (IC₅₀ = 25 ± 5 μM), endowed with a free amino group, can be easily modified. As a result, we chose compound 1f as a starting core for further optimization.

To increase the potency and selectivity of compound 1f for RPTPβ, we sought to introduce molecular diversity to the phenyl ring at the 2-position of the hydroxyindole carboxylic

acid core in order to engage peripheral binding pockets adjacent to the active site (Fig. 1). As discussed earlier, the rationale originates from our earlier observations that diversity elements appended to the β-position of the core enhance both inhibitor potency and selectivity (35, 38, 42), likely through added interactions with secondary binding pockets adjacent to the PTP active site. However, the enhancement in binding affinity through this approach has been rather modest, likely due to the rigidity of the triazole linker formed as a result of the Click reaction. Indeed, no significant contact was observed between the triazole linker and the PTPs (35, 38). Here, we decided to employ amide chemistry, because amide bond formation is one of the most efficient and reliable methods for library constructions, and it enables the use of the most common and commercially available amines and carboxylic acids as reactants. In addition, amide chemistry can be carried out in solution in the absence of deleterious reagents, thus enabling direct screening and identification of hits from the library. Finally, appropriately structured amide linker may impart flexibility that is necessary for optimal interactions with the enzyme.

As shown in Figure 2, compound 2 methyl 4-(dimethylamino)-2-hydroxy-5-iodobenzoate (36, 37) was coupled with the corresponding alkynes 3a-c by Sonogashira coupling to afford compound 4a-c in high yield. Electrophilic cyclizations of 4a-c by I₂ provided iodides 5a-c in 85%–95% yield. After hydrolysis of 5a-c in 5% LiOH for 2 days, 6a-c was obtained. 6a-c was treated with 10% of trifluoroacetic acid (TFA) in dichloromethane (DCM) for 1 h to afford 7a-c by high performance liquid chromatography (HPLC) in 35%–40% yield with more than 95% purity. Compounds 7a-c each contain an amine linker with a different length, attached to the meta-position of the phenyl group at the 2-position of the indole ring. A structurally diverse and commercially available set of 162 carboxylic acids were tethered to 7a-c to generate three focused libraries aimed at capturing additional interactions with adjacent pockets surrounding the active site. The amide libraries 8a-c were assembled in 96-well plates in the presence of HOBt, HBTU, and DIPEA in DMF. The reactions were randomly monitored by liquid chromatography–mass spectrometry (LC-MS). The products were determined to be at least 60%–80% yield and were used directly for screening without further purification.

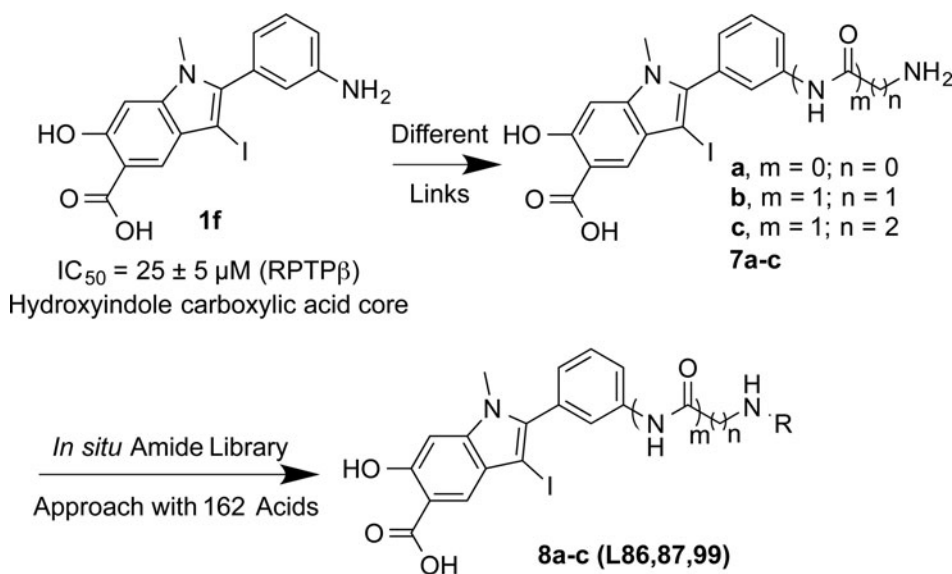
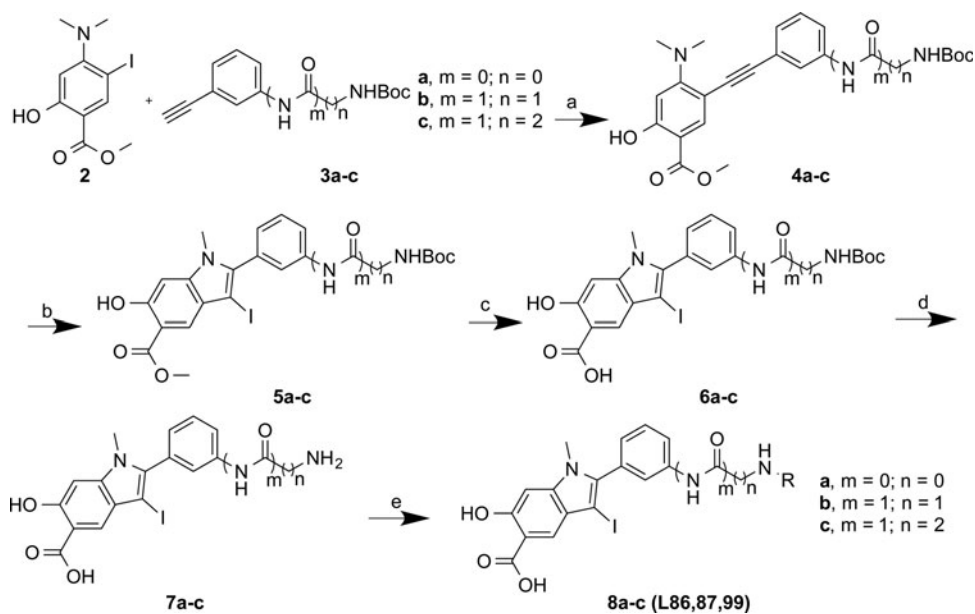


FIG. 1. Strategy and design of hydroxyindole carboxylic acid-based RPTPβ inhibitor. RPTPβ, receptor-type tyrosine protein phosphatase beta.

FIG. 2. Design and synthesis of hydroxyindole carboxylic acid-based library 8a-c. Conditions: (a) corresponding Phenylacetylene, Pd(PPh₃)₂Cl₂, CuI, Et₃N, DMF, 40%–70%; (b) I₂, CH₂Cl₂, NaHCO₃ rt, 85%–95%; (c) 5% LiOH, MeOH/THF/H₂O, rt, 48 h, 80%–85%; (d) 10% TFA in DCM, rt, 1 h, 35%–40%; (e) 162 acids, HOBT, HBTU, DIPEA, DMF, rt, overnight, 60%–80%. rt, room temperature; TFA, trifluoroacetic acid; DCM, dichloromethane; DMF, dimethyl formamide.



The ability of the library compounds to inhibit the RPTP β -catalyzed hydrolysis of pNPP was assessed *in situ* at 10 μ M. The linker size appears to be of significant importance because of the hits identified from the screen; the majority (24) were from library **8b**, only five were from **8a**, and none were from **8c**. These initial hits were resynthesized, purified and their IC₅₀ values for RPTP β were determined (Tables 2 and 3). The most potent compound **8b-1** (L87B44), bearing a 3-bromo-5-iodo substituted phenyl, has an IC₅₀ value of 0.38 \pm 0.02 μ M for RPTP β . Moreover, compound **8b-1** is 11 times more potent than the other di-halogen substituted phenyl molecules (*e.g.*, **8b-7**, **8b-13**, and **8b-21**). 3-Bromo or iodo substituted compounds are thrice more potent than 4-bromo or iodo substituted analogues. For example, we could compare **8b-15** (IC₅₀ = 7.0 μ M) versus **8b-23** (IC₅₀ = 32.0 μ M) and **8b-17** (IC₅₀ = 8.0 μ M) versus **8b-22** (IC₅₀ = 28.0 μ M). The IC₅₀ values of the hits from library **8a** range from 3.0 to 5.4 μ M. Interestingly, compounds **8b-1** and **8a-4** have the same 3-bromo-5-iodo-benzamido scaffold but different linkers; however, compound **8b-1** is 12 times more potent than **8a-4** (IC₅₀ = 0.38 μ M vs. 4.6 μ M). We can draw the conclusion that both a proper linker and a scaffold can significantly influence the binding affinity of RPTP β inhibitors.

Further kinetic analysis indicated that **8b-1** is a reversible and noncompetitive inhibitor for RPTP β with a K_i of 0.48 \pm 0.08 μ M (Fig. 3). Selectivity profiling showed that compound **8b-1** displays more than 14-fold selectivity for RPTP β over 18 other PTPs, including receptor-like PTPs, CD45, PTP μ , LAR PTP ϵ , DEP1, PTP σ , and PTP γ , cytosolic PTPs, PTP1B, FAP-1, SHP2, PTP-PEST, and PTP-MEG2, the *Yersinia* PTP YopH, the CTD phosphatase SSu72, and the dual specificity phosphatase VHR, MKP5, VHZ, and Laforin (Table 4). Together, the results show that **8b-1** is among the most potent and specific of the RPTP β inhibitors reported to date.

Given the excellent potency and selectivity of **8b-1** toward RPTP β , we proceeded to evaluate its cellular efficacy. It has been reported that RPTP β can suppress Met functions by inhibiting the Met-induced Erk1/2 phosphorylation in HEK293 cells (34). To assess the ability of compound **8b-1** to block the

activity of RPTP β inside the cell, we examined the effect of compound **8b-1** treatment on phospho-Erk1/2 signaling in HEK293 cells. Briefly, RPTP β or vector-expressing HEK293 cells were starved overnight and treated with compound **8b-1** for 2 h, followed by stimulation with 10 ng/ml hepatocyte growth factor (HGF) for 30 min, or left unstimulated. Cell lysates were resolved by sodium dodecyl sulfate-polyacrylamide gel electrophoresis (SDS-PAGE), and the levels of phospho-Erk1/2 were examined. As shown in Figure 4A, overexpression of RPTP β reduces the phospho-Erk1/2 level, which is consistent with the reported finding that RPTP β reduced HGF-induced Erk1/2 activation. As expected, treatment with RPTP β inhibitor **8b-1** led to a concentration-dependent enhancement in Erk1/2 phosphorylation level (1.6 \pm 0.1 and 1.8 \pm 0.2-fold increase, respectively, at 0.2 and 0.4 μ M compound **8b-1** concentrations). We also determined the optimal time required for the compound to take effect. RPTP β -expressing cells were treated with 0.4 μ M **8b-1** for various times, and then stimulated with 10 ng/ml HGF for 30 min. As shown in Figure 4B, the treatment of cells with **8b-1** for 1 h leads to 1.5 \pm 0.2-fold increase in Erk1/2 phosphorylation. The enhancement of Erk1/2 phosphorylation peaks (1.8 \pm 0.1-fold) after treatment for 2 h, while prolonged treatment (3 h) only results in a modest increase in Erk1/2 activation (1.3 \pm 0.1-fold). Finally, to ensure that the cellular activity displayed by **8b-1** is not due to nonspecific effects, a structurally related but inactive compound **7b** (Table 2, Core 87, IC₅₀ of 94 μ M against RPTP β) was also evaluated. As expected, compound **7b** showed no measurable effect on Erk1/2 activation (Fig. 4B, Lane 8) when it was incubated with RPTP β -expressing cells for 2 h.

To determine whether **8b-1** could inhibit endogenous RPTP β activity, we surveyed a number of tumor cell lines for RPTP β expression. We found that RPTP β is endogenously expressed in human metastatic breast adenocarcinoma MDA-MB-468 cells (Fig. 5A). To examine the effect of **8b-1** on Erk1/2 activation, MDA-MB-468 cells were serum starved overnight and treated with compound **8b-1** or a negative control **7b** for 2 h, followed by stimulation with 10 ng/ml HGF for 30 min.

TABLE 2. IC₅₀ VALUES (μM) OF HITS IDENTIFIED FROM LIBRARY 8B (L87) FOR RPTP β

ID	R ²	IC ₅₀ (μM)	ID	R ²	IC ₅₀ (μM)
7b (Core 87)	H	94			
8b-1 (L87B44)		0.38 ± 0.02	8b-13 (L87B42)		6.1 ± 0.8
8b-2 (L87A87)		1.99 ± 0.06	8b-14 (L87A60)		6.4 ± 1.7
8b-3 (L87A72)		2.2 ± 0.2	8b-15 (L87A51)		7.0 ± 0.8
8b-4 (L87A61)		2.7 ± 0.1	8b-16 (L87A43)		7.8 ± 0.8
8b-5 (L87B34)		3.4 ± 0.3	8b-17 (L87A12)		8.0 ± 1.0
8b-6 (L87A57)		3.4 ± 0.4	8b-18 (L87A52)		8.0 ± 1.0
8b-7 (L87B39)		4.3 ± 0.2	8b-19 (L87B02)		8.2 ± 1.5
8b-8 (L87A59)		4.9 ± 0.1	8b-20 (L87A88)		9.6 ± 1.6
8b-9 (L87A53)		5.1 ± 0.2	8b-21 (L87A54)		14.5 ± 7.0
8b-10 (L87A27)		5.2 ± 0.5	8b-22 (L87B09)		28.0 ± 4
8b-11 (L87A79)		5.3 ± 0.6	8b-23 (L87B05)		32.0 ± 4
8b-12 (L87B16)		5.6 ± 0.4	8b-24 (L87A66)		40 ± 20

The IC₅₀ values for RPTP β were evaluated at pH 7.0 and 25°C using *p*NPP as a substrate.

Cell lysates were collected and resolved by SDS-PAGE, Phospho-Erk1/2 and total Erk1/2 level were determined by western blot. As shown in Figure 5B, treatment with RPTP β inhibitor **8b-1** increased Erk1/2 activation in a dose-dependent manner (1.57 ± 0.01 and 1.71 ± 0.07-fold increase at 0.4 and 0.8 μM inhibitor **8b-1** concentration), while 0.8 μM **7b** had no effect on Erk1/2 activation, again suggesting that **8b-1** specifically inhibits RPTP β activity and enhances HGF-induced Erk1/2 activation.

To further evaluate the effect of **8b-1** on RPTP β -mediated cellular events in a more physiological setting, we note that RPTP β expression is restricted to endothelial cells (3). In ad-

dition, RPTP β has been shown to play a role in vascular endothelial growth factor (VEGF)/VEGFR signaling (13), and RPTP β phosphatase activity is required for the de-activation of VEGFR-induced downstream Erk1/2 and Akt signaling pathways (23). To investigate whether RPTP β inhibitor **8b-1** could enhance VEGFR signaling, we measured the VEGF-induced Erk1/2 and Akt activation in the presence of **8b-1** in human umbilical vein endothelial cells (HUVECs). HUVECs were serum starved overnight and treated with compound **8b-1** for 2 h, followed by stimulation with 20 ng/ml VEGF for 30 min. Cell lysates were collected and resolved by SDS-PAGE; phospho-Erk1/2 and phospho-Akt levels and total

TABLE 3. IC₅₀ VALUES (μ M) OF HITS FROM LIBRARY 8a (L86) FOR RPTP β

ID	R ³	IC ₅₀ (μ M)
7a (Core 86)	H	25.9 \pm 5.8
8a-1 (L86A45)		3.0 \pm 0.1
8a-2 (L86B34)		3.1 \pm 0.2
8a-3 (L86A53)		4.2 \pm 0.3
8a-4 (L86B44)		4.6 \pm 0.6
8a-5 (L86A37)		5.4 \pm 0.3

The IC₅₀ values for RPTP β were evaluated at pH 7.0 and 25°C using pNPP as a substrate.

Erk1/2 and Akt levels were determined by western blot. As shown in Figure 5C, treatment with RPTP β inhibitor **8b-1** at 0.4 μ M leads to a 1.23 \pm 0.08-fold increase in Akt activation and a 1.57 \pm 0.04-fold increase in Erk1/2 activation, and this fold increase enlarged to 1.78 \pm 0.25-fold for Akt activation and 2.18 \pm 0.01-fold for Erk1/2 activation when **8b-1** concentration was increased to 0.8 μ M, suggesting that **8b-1** significantly

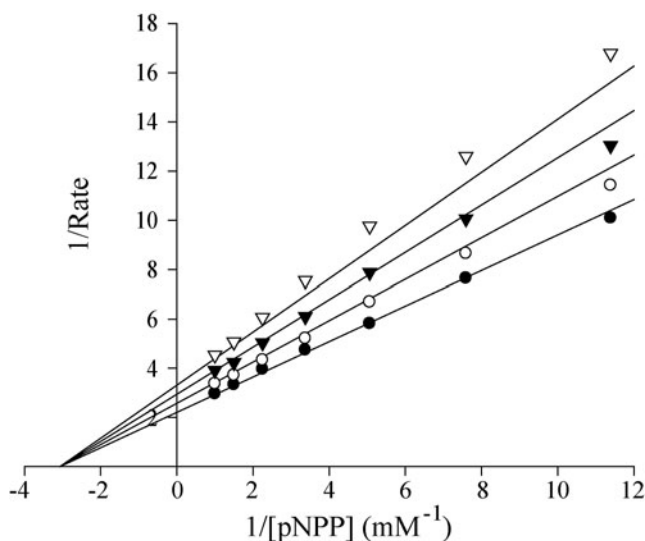


FIG. 3. Lineweaver-Burk plot for Compound **8b-1** (L87B44) mediated RPTP β inhibition. Compound **8b-1** concentrations were 0 (\bullet), 0.1 μ M (O), 0.2 μ M (\blacktriangledown), and 0.3 μ M (∇), respectively.

TABLE 4. SELECTIVITY OF **8b-1** (L87B44) AGAINST A PANEL OF PTPs

PTP	IC ₅₀ (μ M)
RPTP β	0.38 \pm 0.02
FAP-1	5.2 \pm 0.3
SHP2	5.6 \pm 0.5
VHR	5.8 \pm 0.4
PTP1B	5.5 \pm 1.6
PTP-PEST	7.4 \pm 1.0
YopH	8.5 \pm 0.8
CD45	8.6 \pm 0.8
PTP-MEG2	8.2 \pm 1.7
MKP5	> 10
SSu72	9.7 \pm 1.2
VHZ	10 \pm 2
PTP μ	15 \pm 2
Laforin	16 \pm 3
LAR	> 25
PTP ϵ	> 25
DEP1	23 \pm 4
PTP σ	32 \pm 2
PTP γ	60 \pm 20

The IC₅₀ values for the PTPs were evaluated at pH 7.0 and 25°C using pNPP as a substrate. The k_{cat} (s^{-1}) and K_m (mM) values for the PTPs at pH 7 and 25°C with pNPP as a substrate are RPTP β (55.3 s^{-1} and 0.18 mM), FAP-1 (5.5 s^{-1} and 0.56 mM), SHP2 (6.7 s^{-1} and 3.6 mM), VHR (1.8 s^{-1} and 5.8 mM), PTP1B (19.9 s^{-1} and 1.6 mM), PTP-PEST (0.32 s^{-1} and 3.2 mM), YopH (24.6 s^{-1} and 2.1 mM), CD45 (5.6 s^{-1} and 4.9 mM), PTP-MEG2 (5.5 s^{-1} and 6.2 mM), MKP5 (1.4 s^{-1} and 12.7 mM), SSu72 (0.42 s^{-1} and 10.9 mM), VHZ (0.10 s^{-1} and 15.4 mM), PTP μ (0.61 s^{-1} and 2.8 mM), Laforin (0.36 s^{-1} and 3.1 mM), LAR (0.32 s^{-1} and 2.3 mM), PTP ϵ (5.3 s^{-1} and 5.8 mM), DEP1 (331 s^{-1} and 2.2 mM), PTP σ (0.31 s^{-1} and 2.3 mM), and PTP γ (16.8 s^{-1} and 5.3 mM).

PTP, protein tyrosine phosphatase.

extended VEGFR activation in a dose-dependent manner. Taken together, the data show that **8b-1** is highly efficacious in cell-based assays, specifically inhibits RPTP β activity, and increases HGF/Met signaling in both HEK293 and MDA-MB-468 cells and VEGF/VEGFR signaling in HUVECs.

Discussion

Protein tyrosine phosphorylation is an essential post-translational modification that modulates the function of proteins involved in many important signaling pathways. PTPs work in concert with PTKs to control the tyrosine phosphorylation status of target proteins. Not surprisingly, the activity of the PTPs is tightly regulated as a part of the cellular mechanisms for controlling the intensity and duration of responses to various stimuli. One important mechanism for the regulation of PTPs involves covalent modification of the PTP active site Cys thiolate group by endogenously produced ROS. Thus, the oxidative inactivation of the PTPs by ROS offers a dynamic mechanism of PTP regulation that can directly impact the level of tyrosine phosphorylation inside the cell. Thus, it is of great interest to understand the roles that

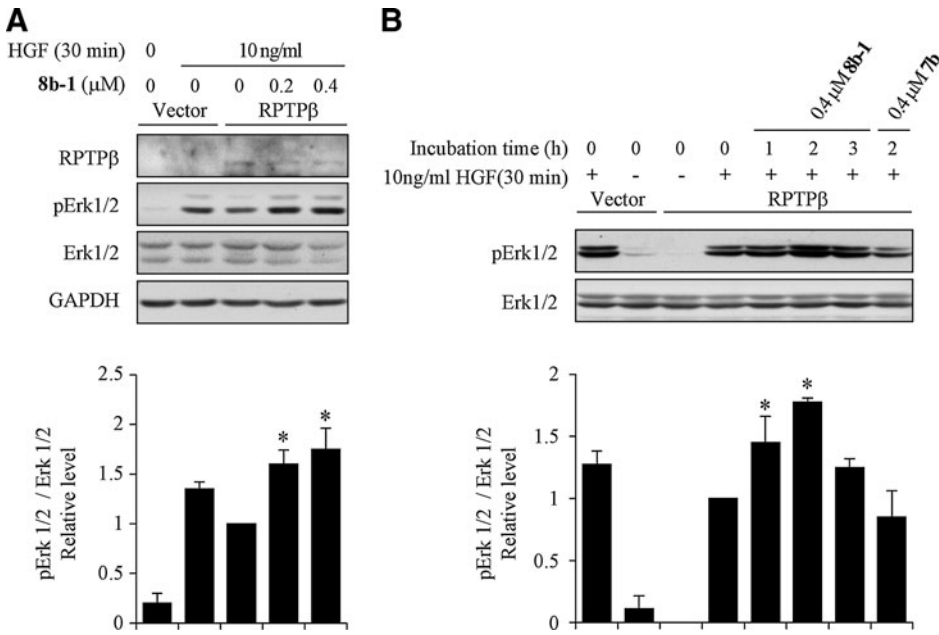


FIG. 4. The cellular activity of compound 8b-1 (L87B44) on HGF-induced Erk1/2 activation in HEK293 cells. (A) Concentration-dependent enhancement of HGF-induced Erk1/2 activation by Compound 8b-1. (B) Time course of compound 8b-1 on HGF-mediated Erk1/2 activation. Bar graph represents the fold change of relative pErk1/2/Erk1/2 level. The results are shown as mean ± SD (n=3). * Represents the significant difference of p<0.05 compared with the control that was stimulated with HGF without compound treatment. HGF, hepatocyte growth factor.

PTPs play in redox signaling. Small-molecule inhibitors can be used as powerful research tools to interrogate the function of the PTPs in redox biology. Unfortunately, there is a general lack of potent, selective, and cell-permeable inhibitors for the PTPs. This study describes a novel approach toward the development of high-affinity and bioavailable PTP inhibitors.

As a proof of concept, we report the most potent and selective inhibitor for RPTPβ, which has been implicated as a potential target for tumor growth and vascular-related diseases. Importantly, the RPTPβ inhibitor 8b-1 possesses highly efficacious cellular activity and inhibits its target in intact cells with similar potencies as those toward the isolated enzyme,

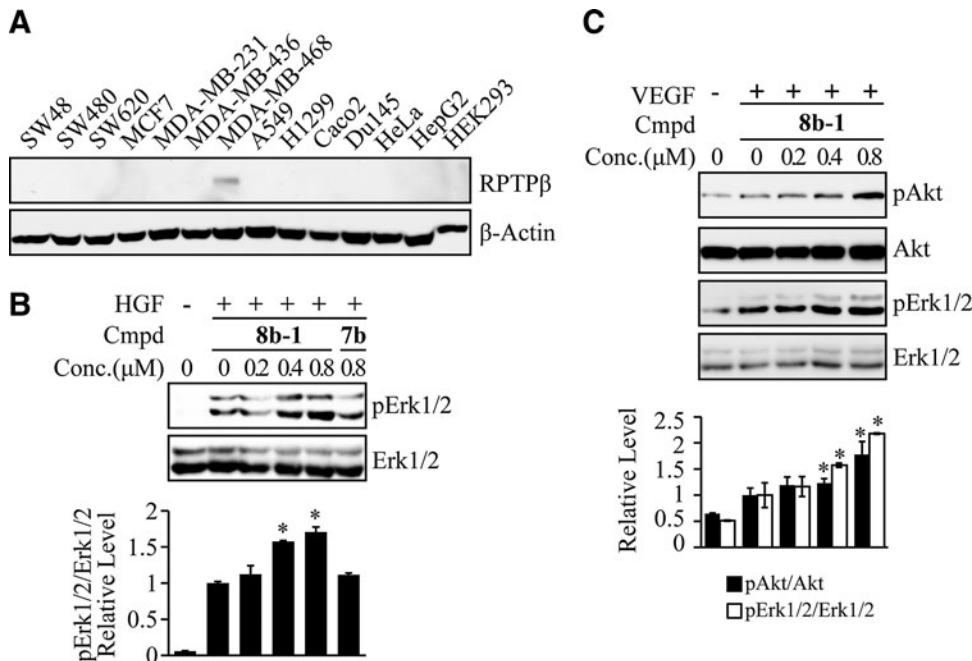


FIG. 5. The cellular activity of compound 8b-1 (L87B44) on cells expressing endogenous PTPβ. (A) Endogenous PTPβ expression pattern in cancer cell lines. (B) Concentration-dependent enhancement of HGF-induced Erk1/2 activation by Compound 8b-1 in MDA-MB-468 cells. Bar graph represents the mean fold change of relative pErk1/2/Erk level. (C) Concentration-dependent enhancement of VEGF-induced Akt and Erk1/2 activation by Compound 8b-1 in HUVECs. Bar graph represents the fold change of relative pAkt/Akt and pErk1/2/Erk1/2 level. The results are shown as mean ± SD (n=3). *Represents the significant difference of p<0.05 compared with the control that was stimulated with growth factor without compound treatment. PTP, protein tyrosine phosphatase; HUVEC, human umbilical vein endothelial cell; VEGF, vascular endothelial growth factor.

whereas previous PTP inhibitors experience 100–10,000-fold loss of potency from biochemical to cellular assays. This inhibitor not only provides a potential lead for tumor and vascular-related diseases but also serves as a useful probe for redox signaling that is regulated by RPTP β .

In conclusion, we report a method that uses an appropriate hydroxyindole carboxylic acid to anchor the inhibitor to the PTP active site and relies on the secondary binding elements introduced through an amide-focused library approach to enhance binding affinity for the target PTP and to impart selectivity against off-target phosphatases. Using the method, we disclose a novel series of hydroxyindole carboxylic acid-based inhibitors for RPTP β , which has been implicated in blood vessel development. The representative RPTP β inhibitor **8b-1** has an IC₅₀ of 0.38 μ M and at least 14-fold selectivity for RPTP β over a large panel of PTPs. Moreover, compound **8b-1** also exhibits excellent cellular activity and can increase HGF-induced Erk1/2 phosphorylation in both HEK293 and MDA-MB-468 cells. Importantly, **8b-1** can also inhibit RPTP β activity and augment VEGF/VEGFR signaling in HUVECs. Thus, compound **8b-1** serves as a promising candidate for the development of novel agents for tumor growth, occlusive cardiovascular disease, vascular leaking syndrome, and other vascular-related diseases. The results give further support that the bicyclic salicylic acid pharmacophore chemistry platform may provide a potential solution to overcome the inhibitor specificity and bioavailability issues that have plagued the PTP drug discovery field for many years. Given the ease and versatility of the amide chemistry-based library approach, we expect that the strategy can be used to identify cell-permeable, potent, and selective inhibitors for other members of the PTP superfamily.

Experimental Section

Materials and general procedures

*p*NPP was purchased from Fluke Co. For organic synthesis, reagents were used as purchased (Aldrich, Acros, Alfa Aesar, TCI), except where noted. ¹H and ¹³C NMR spectra were obtained on Bruker 500 spectrometers with TMS or residual solvent as a standard. All column chromatography was performed using Dynamic Adsorbents 230–400 mesh silica gel (SiO₂) with the indicated solvent system unless otherwise noted. TLC analysis was performed using 254 nm glass-backed plates and visualized using UV light (254 nm); low-resolution mass spectra and purity data were obtained using an Agilent Technologies 6130 Quadrupole LC/MS. High-resolution mass spectrum data were collected on Agilent 6520 Accurate-Mass Q-TOF LC/MS. HPLC purification was carried out on a Waters Delta 600 that was equipped with a Sunfire Prep C18 OBD column (30 × 150 mm, 5 μ m) with methanol-water (both containing 0.1% TFA) as a mobile phase. The preparative HPLC gradient started at 50% methanol in water and ended at 100% methanol after 40 min with 0.1% of TFA. The purity of all final tested compounds was established to be >95% by Agilent Technologies 6130 Quadrupole LC/MS (UV, λ = 254 nm). To analyze compound purity, the analytical HPLC gradient started at 0% methanol in water and ended at 100% methanol after 8 min with 0.1% of TFA. Details on compound synthesis and characterization are described in Supplementary Data (Supplementary Data are available online at www.liebertpub.com/ars).

Protein expression and purification

Briefly, RPTP β was used to transform into *Escherichia coli* BL21/DE3 and grown in LB medium containing 50 μ g/ml kanamycin at 37°C to an OD₆₀₀ of 0.4. After the addition of IPTG to a final concentration of 20 μ M, the culture was incubated at 20°C with shaking for an additional 16 h. The cells were harvested by centrifugation at 5000 rpm for 5 min at 4°C. The bacterial cell pellets were resuspended in 20 mM Tris, pH 7.9, 500 mM NaCl, and 5 mM imidazole, and were lysed by passage through a French press cell at 1200 psi twice. Cellular debris was removed by centrifugation at 16,000 rpm for 30 min at 4°C. The protein was purified from the supernatant using standard procedures of Ni-nitrilotriacetic acid-agarose (Qiagen) affinity purification. The protein eluted from Ni-NTA column was concentrated with an Amicon Ultra centrifugal filter device (Millipore), and the buffer was changed to 20 mM Tris, pH 7.5, 150 mM NaCl, 1 mM EDTA, and 1 mM DTT. Protein concentration was determined using the Bradford dye binding assay (Bio-Rad) diluted according to the manufacturer's recommendations with bovine serum albumin as a standard. The purified RPTP β were made to 30% glycerol and stored at –20°C.

Inhibition study

The inhibition assays were performed at 25°C in 50 mM 3,3-dimethylglutarate buffer, pH 7.0, containing 1 mM EDTA with an ionic strength of 0.15 M adjusted by NaCl. The salicylic acid-based library was screened in a 96-well format at a 10 μ M compound concentration. The reaction was started by the addition of 50 μ l of the enzyme (20 nM) to 150 μ l of reaction mixture containing the final *K_m* value of *p*NPP and various concentrations of the inhibitor in a 96-well plate. The reaction was quenched after 2 min by the addition of 50 μ l of 5 N NaOH, and then, this reaction mixture was detected for absorbance at 405 nm by a Spectra MAX340 microplate spectrophotometer (Molecular Devices). IC₅₀ values were calculated by fitting the absorbance at 405 nm versus inhibitor concentration to the following equation:

$$A_1/A_0 = IC_{50}/(IC_{50} + [I]),$$

where *A*₁ is the absorbance at 405 nm of the sample in the presence of inhibitor; *A*₀ is the absorbance at 405 nm in the absence of inhibitor; and [I] is the concentration of the inhibitor.

The inhibition constants (*K_i*) for the inhibitor for RPTP β were determined at pH 7.0 and 25°C. The mode of inhibition and *K_i* value were determined in the following manner. At various fixed concentrations of the inhibitor, the initial rate at a series of *p*NPP concentrations was measured by following the production of *p*-nitrophenol as describe earlier, ranging from 0.4- to 5-fold of the apparent *K_m* values. The data were fitted to appropriate equations using SigmaPlot-Enzyme Kinetics to obtain the inhibition constant and to assess the mode of inhibition.

For selectivity studies, the PTPs, including the catalytic domains of FAP-1, PTP1B, SHP2, VHR, PTP-PEST, PTP-MEG2, YopH, CD45, VHZ, SSu72, LAR, PTP ϵ , Laforin, DEP1, PTP μ , PTP σ , PTP γ , and MKP5, were expressed and purified from *E. coli*. The inhibition assay for these PTPs was performed under the same conditions (pH 7.0 and 25°C) as

RPTP β , except using a different pNPP concentration corresponding to the K_m of the PTP studied.

Cell culture and immunoblot analysis

HEK293 cells were cultured at 37°C and 5% CO₂ in Dulbecco's-modified Eagle's medium (DMEM) (Corning) that was supplemented with 10% fetal bovine serum (FBS) (HyClone). pShuttle mammalian expression vector subcloned with full-length human RPTP β cDNA (a kind gift from Dr. Yiru Xu in the University of Michigan) or the empty vector was transfected into HEK293 cells using Lipofectamine 2000 (Invitrogen). For biochemical studies, 24 h post-transfection, cells were serum starved overnight followed by treatment with vehicle or compound **8b-1** for an indicated time, and then left either stimulated or unstimulated with 10 ng/ml HGF (Sigma) for 30 min. MDA-MB-468 cells were grown in DMEM that was supplemented with 10% FBS, 50 units/ml penicillin, and 50 μ g/ml streptomycin to 80% confluence, starved with serum-free medium overnight followed by treatment with vehicle, compound **8b-1** or **7b** for 2 h, and then left either stimulated or unstimulated with 10 ng/ml HGF (Sigma) for 30 min. HUVECs were maintained in EBM-2 medium (Lonza) that was supplemented with endothelial growth medium 2 (EGM-2) kit (FCS, hydrocortisone, hFGF-B, VEGF, R3-IGF-1, ascorbic acid, hEGF, GA-1000, and heparin), according to the manufacturer's instructions, then serum starved overnight followed by treatment with vehicle or compound **8b-1** for 2 h, and left either stimulated or unstimulated with 20 ng/ml VEGF for 30 min. Cells were lysed in lysis buffer [1.0% Nonidet P-40, 50 mM Tris-HCl (pH 7.4), 150 mM NaCl, 5 mM EDTA, 2 mM NaVO₃, and 10 mM NaF] plus a protease inhibitor mixture (Roche) and clarified in a microcentrifuge. Lysates were electrophoresed on a 10% polyacrylamide gel, transferred to a nitrocellulose membrane, and probed with antiphospho-Erk1/2 (Cell Signaling), anti-Erk1/2 (Cell Signaling), antiphospho-Akt (Cell signaling), anti-Akt (Cell signaling), anti-GAPDH (Santa Cruz), and anti-PTP β (Santa Cruz) followed by incubation with horseradish peroxidase-conjugated secondary antibodies. The blots were developed by the enhanced chemiluminescence technique using the SuperSignal West Pico Chemiluminescent substrate (Pierce). Data shown are a representation of multiple repeat experiments.

Acknowledgment

This work was supported in part by the National Institutes of Health Grant RO1CA152194 to Z.-Y.Z.

Author Disclosure Statement

No competing financial interests exist.

References

1. Amarasinghe KKD, Evidokimov AG, Xu K, Clark CM, Maier MB, Srivastava A, Colson AO, Gerwe GS, Stake GE, Howard BW, Pokross ME, Graya JL, and Peters KG. Design and synthesis of potent, non-peptidic inhibitors of HPTP β . *Bioorg Med Chem Lett* 16: 4252–4256, 2006.
2. Barrett WC, DeGnore JP, Keng YF, Zhang ZY, Yim MB, and Chock PB. Roles of superoxide radical anion in signal transduction mediated by reversible regulation of protein-tyrosine phosphatase 1B. *J Biol Chem* 274: 34543–34546, 1999.
3. Baumer S, Keller L, Holtmann A, Funke R, August B, Gamp A, Wolburg H, Wolburg-Buchholz K, Deutsch U, and Vestweber D. Vascular endothelial cell-specific phosphotyrosine phosphatase (VE-PTP) activity is required for blood vessel development. *Blood* 107: 4754–4762, 2006.
4. Bova MP, Mattson MN, Vasile S, Tam D, Holsinger L, Bremer M, Hui T, McMahon G, Rice A, and Fukuto JM. The oxidative mechanism of action of ortho-quinone inhibitors of protein-tyrosine phosphatase alpha is mediated by hydrogen peroxide. *Arch Biochem Biophys* 429: 30–41, 2004.
5. Carr AN, Davis MG, Eby-Wilkens E, Howard BW, Towne BA, Dufresne TE, and Peters KG. Tyrosine phosphatase inhibition augments collateral blood flow in a rat model of peripheral vascular disease. *Am J Physiol Heart Circ Physiol* 287: 268–276, 2004.
6. Chae JK, Kim I, Lim ST, Chung MJ, Kim WH, Kim HG, Ko JK, and Koh GY. Coadministration of angiotensin-1 and vascular endothelial growth factor enhances collateral vascularization. *Arterioscler Thromb Vasc Biol* 20: 2573–2578, 2000.
7. Cohen P and Alessi DR. Kinase drug discovery—what's next in the field? *ACS Chem Biol* 8: 96–104, 2013.
8. De Munter S, Kohn M, and Bollen M. Challenges and opportunities in the development of protein phosphatase-directed therapeutics. *ACS Chem Biol* 8: 36–45, 2013.
9. Denu JM and Tanner KG. Specific and reversible inactivation of protein tyrosine phosphatases by hydrogen peroxide, evidence for a sulfenic acid intermediate and implications for redox regulation. *Biochemistry* 37: 5633–5642, 1998.
10. Dominguez MG, Hughes VC, Pan L, Simmons M, Daly C, Anderson K, Noguera-Troise I, Murphy AJ, Valenzuela DM, Davis S, Thurston G, Yancopoulos GD, and Gale NW. Vascular endothelial tyrosine phosphatase (VE-PTP)-null mice undergo vasculogenesis but die embryonically because of defects in angiogenesis. *Proc Natl Acad Sci USA* 104: 3243–3248, 2007.
11. Fachinger G, Deutsch U, and Risau W. Functional interaction of vascular endothelial-protein-tyrosine phosphatase with the Angiotensin receptor Tie-2. *Oncogene* 18: 5948–5953, 1999.
12. Gale NW and Yancopoulos GD. Growth factors acting via endothelial cell-specific receptor tyrosine kinases: VEGFs, angiotensins, and ephrins in vascular development. *Genes Dev* 13: 1055–1066, 1999.
13. Hayashi M, Majumdar A, Li X, Adler J, Sun Z, Vertuani S, Hellberg C, Mellberg S, Koch S, Dimberg A, Koh GY, Dejana E, Belting HG, Affolter M, Thurston G, Holmgren L, Vestweber D, and Claesson-Welsh L. VE-PTP regulates VEGFR2 activity in stalk cells to establish endothelial cell polarity and lumen formation. *Nat Commun* 4: 1672, 2013.
14. Heneberg P, Dráberová L, Bambousková M, Pompach P, and Dráber P. Down-regulation of protein-tyrosine phosphatases activates an immune receptor in the absence of its translocation into lipid rafts. *J Biol Chem* 285: 12787–12802, 2010.
15. Huang P, Ramphal J, Wei J, Liang C, Jallal B, McMahon G, and Tang C. Structure-based design and discovery of novel inhibitors of protein tyrosine phosphatases. *Bioorg Med Chem* 11: 1835–1849, 2003.
16. Hunter T. Tyrosine phosphorylation: thirty years and counting. *Curr Opin Cell Biol* 21: 140–146, 2009.

17. Julien SG, Dubé N, Hardy S, and Tremblay ML. Inside the human cancer tyrosine phosphatome. *Nat Rev Cancer* 11: 35–49, 2011.
18. Kaplan R, Morse B, Huebner K, Croce C, Howk R, Ravera M, Ricca G, Jaye M, and Schlessinger J. Cloning of three human tyrosine phosphatases reveals a multigene family of receptor-linked protein-tyrosine-phosphatases expressed in brain. *Proc Natl Acad Sci USA* 87: 7000–7004, 1990.
19. Karisch R, Fernandez M, Taylor P, Virtanen C, St-Germain JR, Jin LL, Harris IS, Mori J, Mak TW, Senis YA, Östman A, Moran MF, and Neel BG. Global proteomic assessment of the classical protein-tyrosine phosphatome and “Redoxome”. *Cell* 146: 826–840, 2011.
20. Lee SR, Kwon KS, Kim SR, and Rhee SG. Reversible inactivation of protein-tyrosine phosphatase 1B in A431 cells stimulated with epidermal growth factor. *J Biol Chem* 273: 15366–15372, 1998.
21. Lund IK, Andersen HS, Iversen LF, Olsen OH, Møller KB, Pedersen AK, Ge Y, Holsworth DD, Newman MJ, Axe FU, and Møller NPH. Structure-based design of selective and potent inhibitors of protein-tyrosine phosphatase β . *J Biol Chem* 279: 24226–24235, 2004.
22. Mali RS, Ma P, Zeng LF, Martin H, Ramdas B, He Y, Sims E, Gosh J, Nabinger S, Li S, Munugalavada V, Craig AW, Bunting KD, Feng GS, Chan RJ, Zhang ZY, and Kapur R. Role of SHP2 phosphatase in KIT-induced transformation: identification of SHP2 as a druggable target in diseases involving oncogenic KIT. *Blood* 120: 2669–2678, 2012.
23. Mellberg S, Dimberg A, Bahram F, Hayashi M, Rennel E, Ameer A, Westholm JO, Larsson E, Lindahl P, Cross MJ, and Claesson-Welsh L. Transcriptional profiling reveals a critical role for tyrosine phosphatase VE-PTP in regulation of VEGFR2 activity and endothelial cell morphogenesis. *FASEB J* 23: 1490–1502, 2009.
24. Meng FG and Zhang ZY. Redox regulation of protein tyrosine phosphatase activity by hydroxyl radical. *Biochim Biophys Acta* 1834: 464–469, 2013.
25. Meng TC, Fukada T, and Tonks NK. Reversible oxidation and inactivation of protein tyrosine phosphatases *in vivo*. *Mol Cell* 9: 387–399, 2002.
26. Noren-Muller A, Reis-Correa I, Prinz H, Rosenbaum C, Saxena K, Schwalbe HJ, Vestweber D, Cagna G, Schunk S, Schwarz O, Schiewe H, and Waldmann H. Discovery of protein phosphatase inhibitor classes by biology-oriented synthesis. *Proc Natl Acad Sci USA* 103: 10606–10611, 2006.
27. Östman A, Hellberg C, and Böhmer FD. Protein-tyrosine phosphatases and cancer. *Nat Rev Cancer* 6: 307–320, 2006.
28. Puius YA, Zhao Y, Sullivan M, Lawrence DS, Almo SC, and Zhang ZY. Identification of a second aryl phosphate-binding site in protein-tyrosine phosphatase 1B: a paradigm for inhibitor design. *Proc Natl Acad Sci USA* 94: 13420–13425, 1997.
29. Tonks NK. Protein tyrosine phosphatases: from genes, to function, to disease. *Nat Rev Mol Cell Biol* 7: 833–846, 2006.
30. Wang Q, Dubé D, Friesen RW, LeRiche TG, Bateman KP, Trimble L, Sanghara J, Pollex R, Ramachandran C, Gresser MJ, and Huang Z. Catalytic inactivation of protein tyrosine phosphatase CD45 and protein tyrosine phosphatase 1B by polyaromatic quinones. *Biochemistry* 43: 4294–4303, 2004.
31. Winderlich M, Keller L, Cagna G, Broermann A, Kamenyeva O, Kiefer F, Deutsch U, Nottebaum AF, and Vestweber D. VE-PTP controls blood vessel development by balancing Tie-2 activity. *J Cell Biol* 185: 657–671, 2009.
32. Wright MB, Seifert RA, and Bowen-Pope DF. Protein-tyrosine phosphatases in the vessel wall differential expression after acute arterial injury. *Arterioscler Thromb Vasc Biol* 20: 1189–1198, 2000.
33. Xu D, Rovira II, and Finkel T. Oxidants painting the cysteine chapel: redox regulation of PTPs. *Dev Cell* 2: 251–252, 2002.
34. Xu Y, Xia W, Baker D, Zhou J, Cha HC, Voorhees JJ, and Fisher GJ. Receptor-type protein tyrosine phosphatase β (RPTP- β) directly dephosphorylates and regulates hepatocyte growth factor receptor (HGFR/Met) function. *J Biol Chem* 286: 15980–15988, 2011.
35. Yu X, Sun JP, He Y, Guo XL, Liu S, Zhou B, Hudmon A, and Zhang ZY. Structure, inhibitor, and regulatory mechanism of Lyp, a lymphoid-specific tyrosine phosphatase implicated in autoimmune diseases. *Proc Natl Acad Sci USA* 104: 19767–19772, 2007.
36. Yue D and Larock RC. Synthesis of 3-iodoindoles by electrophilic cyclization of N,N-dialkyl-2-(1-alkynyl)anilines. *Org Lett* 6: 1037–1040, 2004.
37. Zeng LF, Xu J, He Y, He R, Wu L, Gunawan AM, and Zhang ZY. A facile hydroxyindole carboxylic acid-based focused library approach for potent and selective inhibitors of mycobacterium protein tyrosine phosphatase B. *ChemMedChem* 8: 904–908, 2013.
38. Zhang X, He Y, Liu S, Yu Z, Jiang ZX, Yang Z, Dong Y, Nabinger SC, Wu L, Gunawan AM, Wang L, Chan RJ, and Zhang ZY. Salicylic acid-based small molecule inhibitor for the oncogenic Src homology-2 domain containing protein tyrosine phosphatase-2 (SHP2). *J Med Chem* 53: 2482–2493, 2010.
39. Zhang ZY. Protein tyrosine phosphatases: prospects for therapeutics. *Curr Opin Chem Biol* 5: 416–423, 2001.
40. Zhang ZY. Protein tyrosine phosphatases: structure and function, substrate specificity, and inhibitor development. *Annu Rev Pharmacol Toxicol* 42: 209–234, 2002.
41. Zhang ZY and Dixon JE. Active site labeling of the Yersinia protein tyrosine phosphatase: The determination of the pK_a of the active site cysteine and the function of the conserved histidine 402. *Biochemistry* 32: 9340–9345, 1993.
42. Zhou B, He Y, Zhang X, Xu J, Luo Y, Wang Y, Franzblau SG, Yang Z, Chan RJ, Liu Y, Zheng J, and Zhang ZY. Targeting mycobacterium protein tyrosine phosphatase B for anti-tuberculosis agents. *Proc Natl Acad Sci USA* 107: 4573–4578, 2010.

Address correspondence to:

Dr. Zhong-Yin Zhang

Department of Biochemistry and Molecular Biology

Indiana University School of Medicine

635 Barnhill Drive

Indianapolis, IN 46202

E-mail: zyzhang@iu.edu

Date of first submission to ARS Central, June 3, 2013; date of final revised submission, October 16, 2013; date of acceptance, November 1, 2013.

Abbreviations Used

DCM = dichloromethane
DIPEA = N,N-diisopropylethylamine
DMEM = Dulbecco's-modified Eagle's medium
DMF = dimethyl formamide
EGM-2 = endothelial growth medium 2
FBS = fetal bovine serum
HBTU = O-(Benzotriazol-1-yl)-N,N,N',N'-tetra-
methyluroniumhexafluorophosphate
HGF = hepatocyte growth factor
HOBT = 1-hydroxybenzotriazol hydrate
HPLC = high performance liquid chromatography
HUVECs = human umbilical vein endothelial cells

LC-MS = liquid chromatography-mass spectrometry
*p*NPP = *p*-nitrophenyl phosphate
PTKs = protein tyrosine kinases
PTPs = protein tyrosine phosphatases
ROS = reactive oxygen species
RPTP β = receptor-type tyrosine protein phosphatase
beta
rt = room temperature
SDS-PAGE = sodium dodecyl sulfate-polyacrylamide
gel electrophoresis
TFA = trifluoroacetic acid
VEGF = vascular endothelial growth factor